Radial decay law for large-scale velocity and magnetic field fluctuations in the solar wind

J. J. Podesta[1]

Received 10 November 2005; revised 20 April 2006; accepted 2 May 2006; published 15 August 2006.

[1] Solar wind data from Helios 1 and 2 and from Voyager 1 and 2 are used to show that between 0.3 and 20 AU in the ecliptic plane, the total energy per unit mass contained in the velocity and magnetic field fluctuations decays approximately as a power law of the form $R^{-\alpha}$, where R is the heliocentric distance in astronomical units (AU) and $-0.64 \leq \alpha \leq -0.41$. It is also shown that to the first order of approximation, this quantity is independent of the effects of solar cycle variations. An analysis of OMNI data at 1 AU from 1969 through 2002 shows that the Alfven ratio, the ratio of kinetic energy to magnetic energy in the fluctuations, exhibits large solar cycle variations rising from 1 or 2 at solar maximum to 8 or 9 either near solar minimum or a couple of years before minimum. This is due to the fact that the kinetic and magnetic energy in the fluctuations both undergo solar cycle variations, with the kinetic energy increasing to a maximum around solar minimum and the magnetic energy decreasing to a minimum around solar minimum. It is found that these effects appear to offset each other so that the sum of the kinetic plus magnetic energies does not exhibit noticeable solar cycle variations.

Citation: Podesta, J. J. (2006), Radial decay law for large-scale velocity and magnetic field fluctuations in the solar wind, *J. Geophys. Res.*, *111*, A08103, doi:10.1029/2005JA011528.

1. Introduction

[2] The most well known property of turbulence in incompressible fluids is the Kolmogorov energy spectrum characterized by a power law exponent equal to $-5/3$ in the inertial range. Another important property is the asymptotic energy decay law

$$E(t) \propto t^{-\alpha}, \tag{1}$$

which describes the free decay of the turbulence after the turbulent forcing is "turned off." In equation (1), E is the average kinetic energy of the fluid, t is the time variable, and α is a constant ($\alpha \sim 1$). A power law decay indicates that the turbulent energy decays very slowly once the forcing is removed; contrary to a smooth laminar velocity field which decays exponentially in time proportional to $\exp(-\nu k^2 t)$, where ν is the kinematic viscosity and k is the magnitude of the Fourier wave number. This is perhaps the oldest and most well known property of incompressible fluid turbulence [*Frisch*, 1995].

[3] Computer solutions (simulations) of the equations of incompressible magnetohydrodynamics (MHD) show that three-dimensional homogeneous isotropic turbulence in an incompressible magnetofluid also decays slowly in time with an approximate energy decay law in the nonzero helicity case of the form

$$E(t) \propto t^{-1/2} \tag{2}$$

and, in the zero helicity case,

$$E(t) \propto t^{-1} \tag{3}$$

[*Biskamp and Müller*, 2000], where E is the total energy—kinetic plus magnetic.

[4] By analogy, large-scale fluctuations in the solar wind are expected to exhibit a radial power law decay of the form $R^{-\alpha}$, where R is the radial distance from the sun in astronomical units (AU). Solar wind velocity and magnetic field fluctuations are freely decaying when separated from their sources in the solar corona and in the solar wind acceleration region. While being swept outward at super-Alfvenic speeds by the solar wind, these fluctuations undergo a radial decay that resembles the free decay of turbulence after the sources driving the turbulence have been removed.

[5] The simulations of *Biskamp and Müller* [2000] do not provide an accurate physical model for the evolution of solar wind turbulence because in the solar wind reference frame the fluctuations are neither incompressible nor isotropic. However, the slow power law decay seen in these simulations is typical of the type of behavior expected in the solar wind. The dynamics of small-scale turbulent motions in the solar wind are approximately incompressible [*Bavassano and Bruno*, 1995; *Goldstein et al.*, 1995], even though they are not isotropic. For this reason, models like

[1]Laboratory for Solar and Space Physics, NASA Goddard Space Flight Center, Greenbelt, Maryland, USA.

0148-0227/06/2005JA011528

that of *Biskamp and Müller* [2000] may be considered to yield a rough first approximation for the evolution of solar wind fluctuations.

[6] The purpose of this study is to use in situ measurements of solar wind plasma and magnetic fields to determine the radial decay law of large-scale fluctuations in the solar wind. This law is fundamental to the physics of solar wind turbulence because these large-scale fluctuations constitute the energy source for the turbulence and, consequently, the energy source for turbulent heating of solar wind plasma. The measurement of this law is difficult because of the sparsity of solar wind data beyond the orbit of the Earth (1 AU). As a consequence, the empirical estimates contain significant uncertainties. In the future when much larger data sets become available the radial decay law will be more amenable to measurement.

[7] In this study, the term ''large-scale fluctuations'' refers to fluctuations with periods of approximately one hour to 27 days (one solar rotation) or more, that is, from approximately 4×10^{-7} Hz to 3×10^{-4} Hz. This terminology was introduced by Burlaga and has been used several times in the literature [*Burlaga*, 1995; *Burlaga et al.* 1989]. For solar wind power spectra, this range of frequencies contains most of the power in the fluctuations. At these scales the fluctuations can be considered compressible consisting of a mixture of both fast and slow wind, shocks, and other structures.

[8] In the ecliptic plane, during the declining phase of the solar cycle and near solar minimum the energy in the large-scale fluctuations is dominated by recurring streams and the large-scale stream structure of the solar wind. During the ascending phase of the solar cycle and near solar maximum the stream structure almost disappears so that the fluctuating power at these frequencies is reduced although it still dominates the power spectrum.

[9] A brief outline of this paper is as follows. A review of previous work is provided in section 2. The analysis procedures and results obtained in this study are described in section 3. The effects of solar cycle variations are discussed in section 4 and the conclusions are presented in section 5.

2. Previous Work

[10] The radial variation of velocity and magnetic field fluctuations in the solar wind have been reviewed by *Roberts and Goldstein* [1991] and by *Roberts et al.* [1990]. Related studies of the radial evolution of solar wind power spectra can be found in work by *Marsch and Tu* [1990a, 1990b]. Further information, including references to some of the theoretical work on this subject, can be found in several comprehensive reviews of solar wind turbulence including those by *Marsch* [1991], *Goldstein et al.* [1995], *Tu and Marsch* [1995], and *Bruno and Carbone* [2005]. More recent theoretical work includes that of *Zank et al.* [1996], *Matthaeus et al.* [1999], and *Cranmer and van Ballegooijen* [2005].

[11] Empirical studies of the radial variation of large-scale fluctuations in the solar wind based on in situ measurements were performed by *Klein et al.* [1987] and by *Roberts et al.* [1990]. The study by *Klein et al.* [1987] considered only magnetic field fluctuations and neither study explicitly estimated the radial variation of the total energy in the fluctuations (kinetic plus magnetic). *Klein et al.* [1987] used one day averages of the magnetic field data from Voyager 1 and Voyager 2 to compute variances in the fluctuations over successive 26 day intervals, approximately one solar rotation. According to their results the RMS power in the large-scale magnetic field fluctuations obeys the radial power law

$$\sigma_{B_R}^2 \simeq aR^{-b}, \tag{4}$$

where $a = 3.82$ (nT)^2, $b = 2.80$, and $1 < R < 20$ AU for Voyager 1, and $a = 4.55$ (nT)^2, $b = 2.82$, and $1 < R < 14$ AU for Voyager 2. Similarly,

$$\sigma_{B_T}^2 \simeq aR^{-b}, \tag{5}$$

where $a = 7.63$ (nT)^2, $b = 2.70$, and $1 < R < 20$ AU for Voyager 1, and $a = 7.57$ (nT)^2, $b = 2.68$, and $1 < R < 14$ AU for Voyager 2. Here, (B_R, B_T, B_N) are the Cartesian components of the magnetic field vector in spacecraft RTN coordinates. Although $\sigma_{B_N}{}^2$ is not provided in their paper it is reasonable to expect, on the basis of this and previous studies, that $\sigma_{B_N}^2 \simeq \sigma_{B_T}^2$. It is important to note that the data used to derive the fits (4) and (5) were not corrected for possible solar cycle variations. Assuming that the average density falls off like R^{-2}, it follows from the results of *Klein et al.* [1987] that the magnetic energy per unit mass decreases approximately like $R^{-0.7}$ from 1 to 20 AU.

[12] *Roberts et al.* [1990] used one hour averaged data obtained between 0.3 and 20 AU by several different spacecraft, including Helios and Voyager, to measure the total power in fluctuations having periods less than or equal to 10 days. Time series for selected data intervals were digitally filtered to isolate the frequency band containing periods less than 10 days and the variance of the fluctuations was then computed from the filtered time series. The results show that at the largest scales studied (10 days) the magnetic field fluctuations roughly obey the WKB relation $\mathrm{var}(\boldsymbol{B}) \propto R^{-3}$ from 0.3 to 2 AU but decrease more slowly than R^{-3}, roughly as R^{-2}, from 2 to ~10 AU (A. Roberts, private communication, 2005). Assuming that the average density falls off like R^{-2}, these results suggest that the magnetic energy per unit mass decreases approximately like R^{-1} from 0.3 to 2 AU and more slowly than R^{-1} from 2 to 10 AU. The Alfvén ratio decreases from around 3 at 0.4 AU to 0.8 at 8 AU and then remains approximately constant from 8 to 20 AU. Consequently, the kinetic energy decreases faster than the magnetic energy between 0.3 and 8 AU. *Roberts et al.* [1990] did not take into account possible effects due to solar cycle variations.

3. Measurement Methods and Results

[13] The kinetic energy per unit mass is defined by the variance of the velocity field

$$E^V(R) = \frac{1}{2}\mathrm{var}\{\boldsymbol{v}(R,t)\} = \frac{1}{2}\left\langle |\boldsymbol{v}(R,t) - \bar{\boldsymbol{v}}(R)|^2 \right\rangle, \tag{6}$$

where $\boldsymbol{v}(R, t)$ is the velocity field, $|\boldsymbol{v}|^2 = v_x^2 + v_y^2 + v_z^2$, $\bar{\boldsymbol{v}}(R) = \langle \boldsymbol{v}(R, t) \rangle$ is the mean velocity at the point R, and the brackets

denote the ensemble average. The stochastic process $\boldsymbol{v}(R, t)$ is assumed to be stationary and ergodic so that, in practice, the ensemble average is computed using a time average. The energy per unit mass contained in the magnetic field fluctuations is defined by

$$E^M(R) = \frac{1}{2}\mathrm{var}\{\boldsymbol{b}(R,t)\} = \frac{1}{2}\left\langle |\boldsymbol{b}(R,t) - \bar{\boldsymbol{b}}(R)|^2 \right\rangle, \quad (7)$$

where

$$\boldsymbol{b}(R,t) = \frac{\boldsymbol{B}(R,t)}{\sqrt{\mu_0 \rho(R,t)}} \quad (8)$$

is the magnetic field expressed in terms of velocity units. In equation (8), $\rho(R, t)$ is the solar wind mass density and μ_0 is the permeability of free space. In this paper SI units are used throughout. The total energy per unit mass contained in the fluctuations is defined by

$$E = E^V + E^M. \quad (9)$$

[14] It is possible to use the average density $\bar{\rho}(R)$ rather than the instantaneous density $\rho(R, t)$ in equation (8). This leads to somewhat smaller values of the magnetic energy per unit mass E^M, although the radial trends are similar in both cases. In general, the variances (6) and (7) depend not only on the radius R but on the heliographic latitude θ. The dependence on latitude is omitted since the observations in this study are confined to the ecliptic plane, that is, within ±7 degrees of the solar equatorial plane.

[15] Ideally, one should measure the total variance (power) in the fluctuations at a discrete sequence of radial points along a particular radial direction, that is, at a fixed heliographic latitude. At each point one should obtain a long time series of measurements spanning several solar cycles (ideally). The variance of the time series then yields the total power in the fluctuations

$$\sigma^2(R) = \int_{-\infty}^{\infty} S(R,f)\, df, \quad (10)$$

where $S(R, f)$ is the power spectrum measured at the radial distance R and f is the frequency in Hertz (Hz). In practice, because the correlation time of the solar wind fluctuations is on the order of 10 hours and most of the power is concentrated at the large scales, it is sufficient to use a sampling rate on the order of one to ten hours. The minimum number of samples required to estimate the variance from the time series data is typically on the order of 10^3 to 10^4.

[16] Unfortunately, existing spacecraft data cannot accommodate the ideal measurement scenario just described. In practice, the spacecraft is always moving rapidly so that one must group the data into radial bins (radial intervals). In the case of Voyager, the spacecraft makes a single pass during its outward bound trajectory so that the dwell time in each radial bin is very limited. The spacecraft is moving with a velocity of approximately 3 AU per year so that for a radial bin size of 1 AU the time spent in each bin is only 1/3 year. This is not long enough to allow a complete sampling of the full range of solar wind conditions over a typical solar cycle. As a consequence, the measurements are statistically inadequate and produce very noisy estimates of the radial dependence of the fluctuating power.

[17] In this study, one hour averages of plasma and magnetic field data were obtained from the NSSDC (merged data sets) for the complete missions of Helios 1, Helios 2, Voyager 1, and Voyager 2. The data for each mission are sorted into radial bins and the variance is computed separately for the data contained in each bin. The data from each spacecraft are processed separately. The data from Helios 1 cover the period from 1975 to 1981, roughly from solar minimum to solar maximum of solar cycle 21. The data from Helios 2 cover the period from 1976 to 1981. For Voyager 1, the plasma instrument failed after 1980 so only data between 1977 and 1981 are analyzed here ($1 < R < 10$ AU). In the case of Voyager 2, only the data from 1977 through 1986 are used so that $1 < R < 20$ AU. This is to ensure the integrity (accuracy and reliability) of the Voyager measurements since the plasma instruments were only designed for $1 < R < 20$ AU [*Bridge et al.*, 1977]. More details of the analysis methods are described below. The results of the analysis are shown in Figures 1 and 2.

3.1. Helios Data

[18] For Helios 1 and Helios 2, the bin size is $dr = 0.1$ AU and the separation between centers of adjacent bins is $dr/4$ so that the bins overlap each other. The mass density ρ of the solar wind is computed from the measured proton number density by assuming a fixed ratio of 24 protons to each alpha particle, $n_p/n_\alpha = 24$, so that $\rho = 1.17 m_p n_p$, where m_p is the proton mass, n_p is the proton number density, and n_α is the number density of alpha particles. If the average mass density in each bin is used instead of the instantaneous density in equation (8), then the values for the magnetic energy per unit mass are found to be smaller than those shown in Figure 1 by a factor of approximately 2/3; more specifically, by factors of between 0.49 and 0.78 for Helios 1 and by factors of between 0.59 and 0.78 for Helios 2. One more detail should be mentioned regarding the analysis of data from Helios 1 and 2, namely, that there are roughly twice as many data points in each velocity bin as in each magnetic field bin; the latter is shown in Figure 1 (bottom). This is because the simultaneous density and magnetic field data needed for each point in the magnetic field bins are less abundant than the number of velocity data points in each bin.

[19] Linear least squares fits to $\log(E)$ versus $\log(R)$ yield the relations

$$E(R) \simeq 6.84 \times 10^3\, R^{-0.61} \quad (\mathrm{km/s})^2, \quad (11)$$

where $0.3 < R < 1$ AU for Helios 1, and

$$E(R) \simeq 6.64 \times 10^3\, R^{-0.52} \quad (\mathrm{km/s})^2, \quad (12)$$

where $0.3 < R < 1$ AU for Helios 2. These are the principal results of the analysis. A linear least squares fit to $\log[\mathrm{var}(\boldsymbol{B})]$ versus $\log(R)$, not shown in Figure 1, yields the relations

$$\mathrm{var}(B) \simeq 39.3\, R^{-2.91} \quad (\mathrm{nT})^2 \quad (13)$$

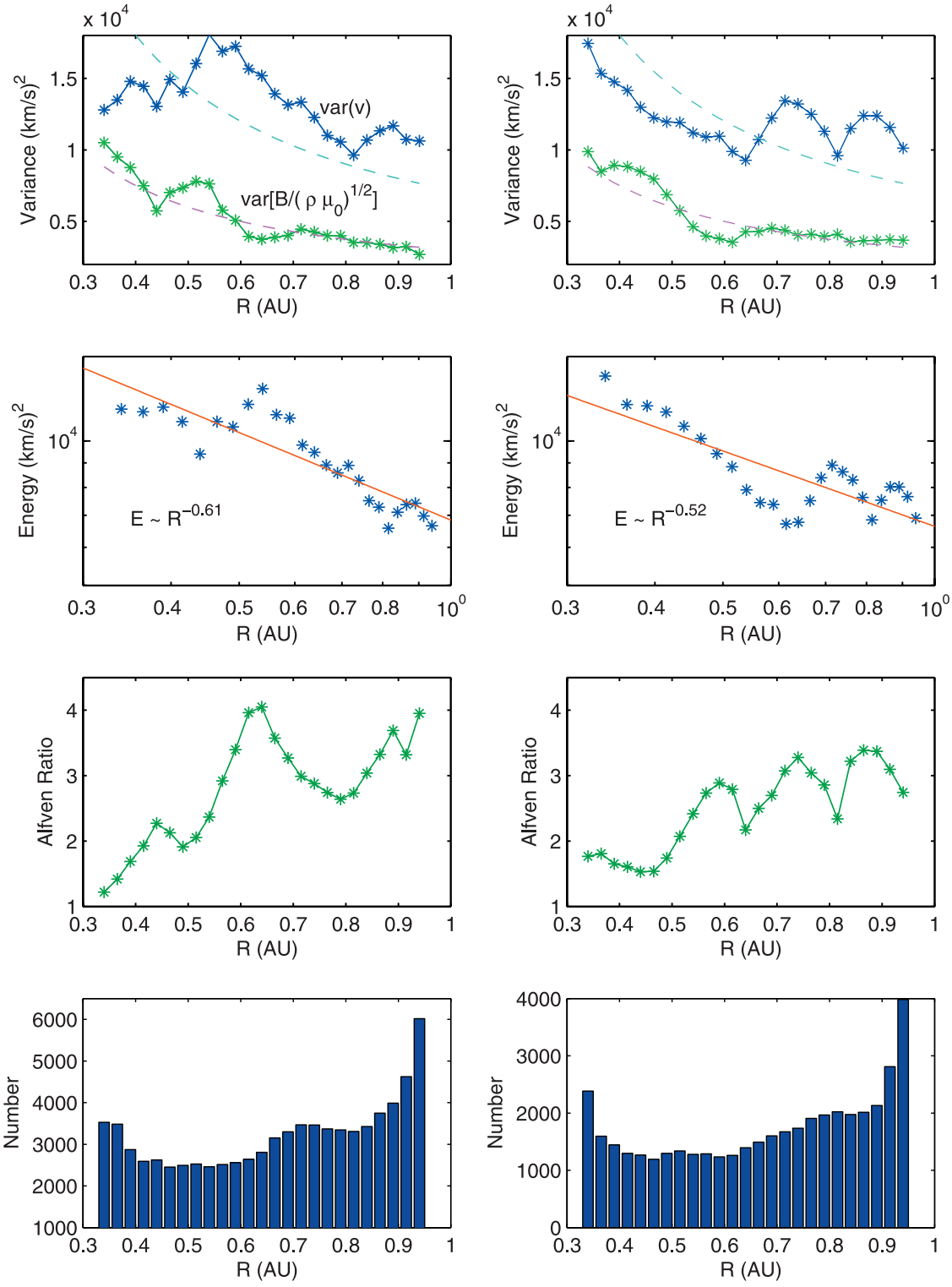

Figure 1. (top) Radial variation of the kinetic and magnetic energies per unit mass, (second from the top) total energy per unit mass, (third from the top) Alfven ratio, and (bottom) number of samples in each magnetic energy bin for (left) Helios 1 and (right) Helios 2. The dashed lines in the top plots are proportional to $1/R$. The lines on the plots for the total energy are the linear least squares fits to $\log(E)$ versus $\log(R)$.

for Helios 1 and

$$\mathrm{var}(B) \simeq 35.2\, R^{-3.13} \quad (\mathrm{nT})^2 \tag{14}$$

for Helios 2, where $0.3 < R < 1$ AU. It is found that the transverse components of the fluctuations in the magnetic field are of the same order of magnitude, $\sigma^2_{B_N} \sim \sigma^2_{B_T} \sim R^2$, whereas the magnitude of the radial component, $\sigma^2_{B_R} \sim R^4$, is

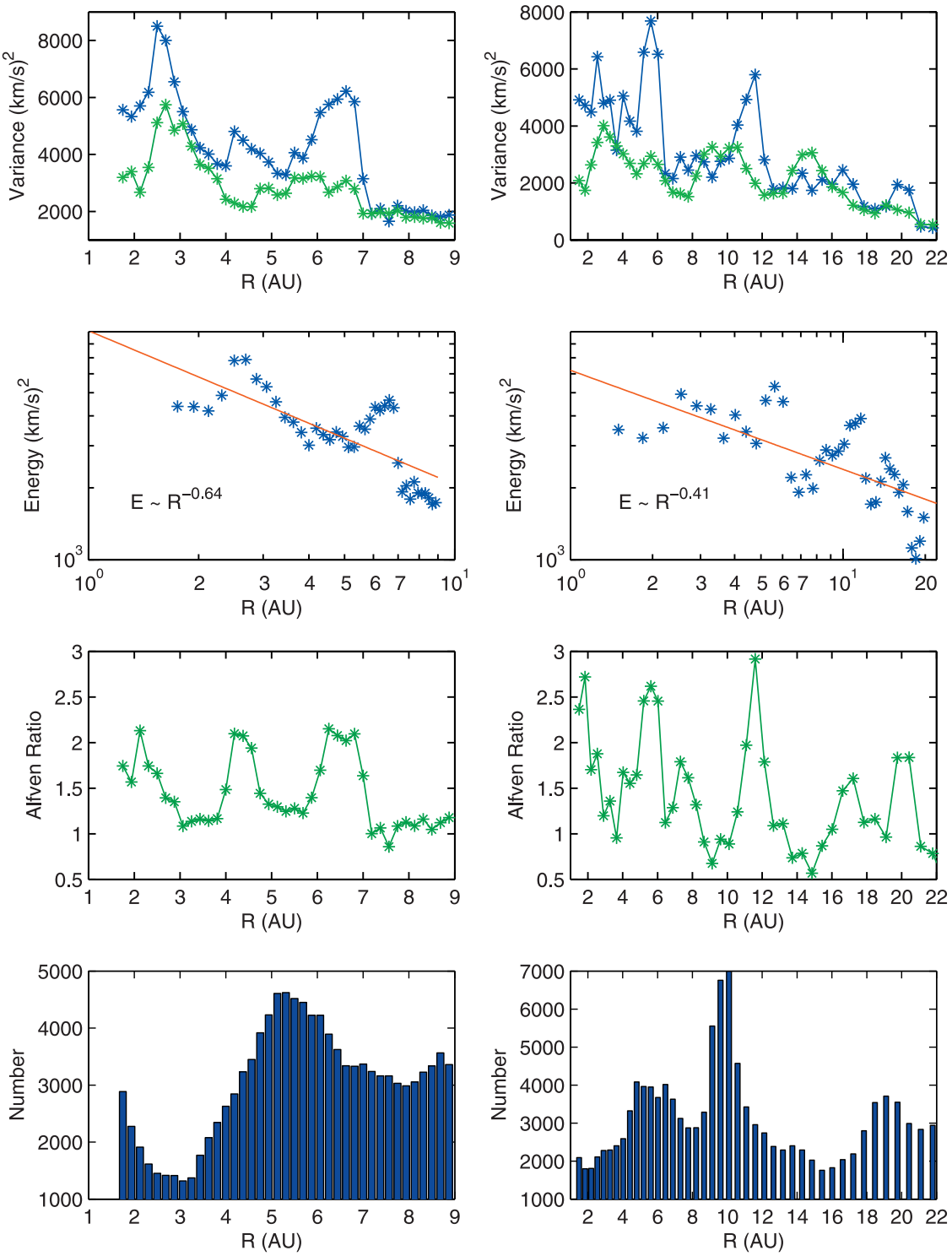

Figure 2. (top) Radial variation of the kinetic (blue) and magnetic (green) energies per unit mass, (second from the top) total energy per unit mass, (third from the top) Alfven ratio, and (bottom) number of samples in each magnetic energy bin for (left) Voyager 1 and (right) Voyager 2. Note that the total energy is drawn on a log-log plot. The lines on the plots for the total energy are the linear least squares fit to $\log(E)$ versus $\log(R)$.

roughly ten times the magnitude of the transverse components at 0.3 AU and then decreases monotonically to become approximately equal to that of the transverse components at 1 AU (the radial dependence seen in the data may be estimated from the empirical relations $|B_R| \sim R^{-2}$ and $|B_T| \sim R^{-1}$ [*Mariani et al.*, 1979] together with the assumptions $|\delta B_R| \sim |B_R|$ and $|\delta B_T| \sim |B_T|$). Assuming a density decrease proportional to R^{-2}, the relations (13) and (14) imply that

the magnetic energy per unit mass decreases roughly as R^{-1} from 0.3 to 1 AU. This is consistent with the empirical data plotted in Figure 1 (top).

[20] For the velocity field, the variance of the radial component is larger than the variance of the transverse components by a factor on the order of 10 throughout the interval from 0.3 to 1 AU. This is due to the radial stream structure of the solar wind and the fact that the radial velocity component dominates the kinetic energy of the flow.

3.2. Voyager Data

[21] For Voyager 1, the radial bin size is $dr = 1.5$ AU and the separation between centers of adjacent bins is $dr/8$. As the speed of the spacecraft is approximately 3.3 AU per year, each radial bin contains data spanning more than six solar rotations. For Voyager 2, the radial bins are chosen to have geometrically increasing bin sizes. This permits more uniform sample sizes at all radial distances since the increasing bin size compensates for the increasing number of data gaps at large distances. The nth radial bin covers the interval (a_n, b_n), where $b_n = a_n + \Delta_n$, $\Delta_n = \delta\lambda^n$, $a_{n+1} = a_n + \alpha\Delta_n$, $a_0 = 1$ AU, and $n = 0, 1, 2, 3, \ldots$ The radial position of the bin is equal to the midpoint of the interval. For the analysis of Voyager 2 data, the values $\delta = 1$ AU, $\alpha = 1/3$, and $\lambda = 1 + (\alpha/19)$ were chosen to obtain bin sizes that increase from 1 AU near $R = 1$ AU to approximately 2 AU near $R = 20$ AU. For both Voyager 1 and 2 the number of data points in the velocity bins are approximately equal to the number of data points in each magnetic field bin, where the latter is shown in Figure 2 (bottom).

[22] Linear least squares fits to $\log(E)$ versus $\log(R)$ yield the relations

$$E(R) \simeq 9.08 \times 10^3 \, R^{-0.64} \quad (\mathrm{km/s})^2, \tag{15}$$

where $1 < R < 10$ AU for Voyager 1, and

$$E(R) \simeq 6.20 \times 10^3 \, R^{-0.41} \quad (\mathrm{km/s})^2, \tag{16}$$

where $1 < R < 20$ AU for Voyager 2. These are the primary results of the analysis. It should be noted that if the average mass density in each bin is used instead of the instantaneous density in equation (8), then it is found that for Voyager 1 the quantity var($\boldsymbol{b}$) is reduced by a factor of roughly 1/2 or, more precisely, by factors ranging between 0.34 and 1.01. Likewise, for Voyager 2, the quantity var($\boldsymbol{b}$) is reduced by a factor of roughly 2/3 or, more precisely, by factors of between 0.57 and 1.05.

[23] Linear least squares fits to $\log[\mathrm{var}(\boldsymbol{B})]$ versus $\log(R)$, not shown in Figure 2, yield the relations

$$\mathrm{var}(\boldsymbol{B}) \simeq 62.3 \, R^{-2.43} \quad (\mathrm{nT})^2, \tag{17}$$

where $1 < R < 10$ AU for Voyager 1, and

$$\mathrm{var}(\boldsymbol{B}) \simeq 50.4 \, R^{-2.26} \quad (\mathrm{nT})^2, \tag{18}$$

where $1 < R < 20$ AU for Voyager 2. In addition, it is found that the variance of all three components of the magnetic field have a similar radial dependence from 1 to 20 AU (each a straight line on a log-log plot). It is found that $\sigma_{B_T}^2$ dominates the power, the magnitude of $\sigma_{B_N}^2$ is smaller than $\sigma_{B_T}^2$ by a factor on the order of 2 or 3, and the magnitude of $\sigma_{B_R}^2$ is smaller than $\sigma_{B_N}^2$ by a factor on the order of 2 or 3. Assuming a density decrease proportional to R^{-2}, the relations (17) and (18) imply that the magnetic energy per unit mass decreases roughly like $R^{-0.35}$ from 1 to 20 AU. This is consistent with the empirical data plotted in Figure 2 (top).

[24] For the velocity field, the variance of the radial component is larger than the variance of the transverse components by a factor on the order of 10 throughout the interval from 1 to 20 AU. This is expected because of the dominant radial stream structure of the solar wind. The variance of the transverse velocity components, the 'T' and 'N' components, are roughly equal in magnitude from 1 to 20 AU.

4. Solar Cycle Variations

[25] In this section it is shown that solar cycle variations do not have a significant effect on the total energy per unit mass in the large-scale fluctuations in the ecliptic plane. The large-scale velocity and magnetic field fluctuations at 1 AU were studied using one hour average data from the OMNI data set. The quantities E^V and E^M were computed over 1/3 year intervals and the calculations were repeated every 1/6 year. The results for the period of the Helios and Voyager missions analyzed in this paper is shown in Figure 3. The analysis of each solar cycle covered by the OMNI data set between 1969 and 2002 shows a similar pattern.

[26] The kinetic and magnetic energies are nearly equal around solar maximum with an Alfvén ratio near 1 or 2. From solar maximum to solar minimum the magnetic energy decreases by a factor on the order of 1/2 or 1/3 while the kinetic energy tends to increase, though less smoothly, by a factor on the order of two or three. Consequently, the Alfvén ratio increases from around 1 or 2 at solar maximum to around 8 or 9 near solar minimum. The increase in the kinetic energy is due to the occurrence of high-speed streams near solar minimum and during the declining phase of the solar cycle, a well known effect which is due to the occurrence of equatorial coronal holes.

[27] It is interesting that although separately the kinetic and magnetic energies E^V and E^M exhibit noticeable solar cycle variations, the total energy E does not exhibit a clearly discernable pattern or trend. Instead, the total energy undergoes fluctuations about its mean value. Even though the relative fluctuations are sometimes large, the overall time variation is trendless. This result is remarkable in light of the large changes in the Alfvén ratio during the solar cycle. Assuming that the solar cycle variations at any heliocentric distance between 0.3 and 20 AU is similar to the variations observed at 1 AU, these results suggest that to the first order of approximation the radial dependence of the total energy E can be estimated from the data without concern for solar cycle effects. However, corrections due to solar cycle effects are important when estimating the radial variation of the Alfvén ratio. Such corrections are not attempted here. As a consequence, the plots of the Alfven ratio in Figure 2 are probably contaminated by solar cycle effects and therefore are untrustworthy, while the plots of the Alfven ratio in

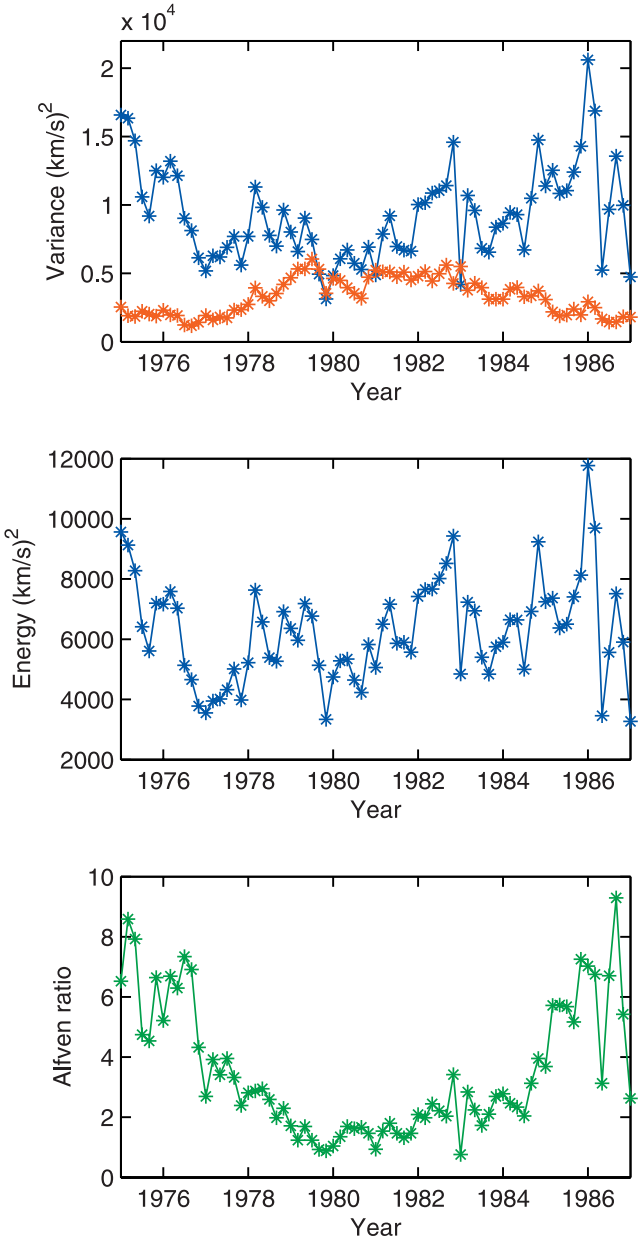

Figure 3. (top) Solar cycle variations of the kinetic (blue) and magnetic (red) energy per unit mass, (middle) total energy per unit mass, and (bottom) the Alfvén ratio as measured at 1 AU. Solar cycle 21 extends from solar minimum in 1975/1976 to solar maximum in 1980 to the succeeding solar minimum in 1986.

Figure 1 are probably less effected because the Helios data set spans a significant portion of the solar cycle.

5. Discussion and Conclusions

[28] The data from Helios and Voyager show that between 0.3 and 20 AU the total energy per unit mass in the fluctuations decays approximately as a power law with an exponent of between -0.41 and -0.64. The scatter in the data is large so that these values contain large uncertainties, but the fact that independent fits obtained from Helios (0.3 to 1 AU) and Voyager data (1 to 20 AU) all yield similar exponents provides confirmation of the general trend. In addition, the amplitudes of all the fits are found to be in rough agreement with each other.

[29] A comparison of the results from Helios with those from Voyager in Figures 1 and 2 shows that from 0.3 to 1 AU the kinetic energy per unit mass decays more gradually than the magnetic energy per unit mass, whereas, from 1 to 20 AU the kinetic energy per unit mass decays more rapidly than the magnetic energy per unit mass—even without corrections for solar cycle effects. This is the most noticeable difference between the radial dependence in the two regions $R < 1$ AU and $R > 1$ AU. One of the primary differences in the solar wind in these two regions is that the solar wind is still undergoing a significant radial acceleration between 0.3 and 1 AU with an average velocity gain on the order of 10%, whereas, beyond 1 or 2 AU the average solar wind velocity is roughly constant. Assuming that the kinetic fluctuations draw energy from the average flow only when the average flow is accelerating, it follows that the kinetic component of the fluctuations should decay more gradually from 0.3 to 1 AU than from 1 AU to 20 AU. This could explain the observed differences in the regions $R < 1$ AU and $R > 1$ AU.

[30] As one can see from Figure 1, between 0.3 and 1 AU the magnetic energy per unit mass decays approximately like $1/R$ and the kinetic energy per unit mass decays more gradually than $1/R$, that is, E^M decays more rapidly than E^V. Between 1 and 20 AU, the magnetic energy per unit mass decays more slowly than $1/R$, approximately like $R^{-1/3}$, and the kinetic energy per unit mass decays more rapidly than the magnetic energy. Thus E^V decays more rapidly than E^M. As a consequence, the Alfvén ratio generally increases in the range $0.3 < R < 1$ AU and decreases in the range $1 < R < 20$ AU. Note, however, that these results are effected by solar cycle variations. In the range $0.3 < R < 1$ AU the magnetic field fluctuations var($\boldsymbol{B}$) decrease approximately like R^{-3} while in the range $1 < R < 20$ AU they decrease approximately like $R^{-2.35}$. The average density decreases approximately like R^{-2} from 0.3 to 20 AU.

[31] The results for the Alfvén ratio presented in Figures 1 and 2 are consistent with those of *Roberts et al.* [1990] which show that at the 10 day scale the Alfvén ratio decreases from values on the order of 2 or 3 between 0.3 and 1 AU to values on the order of unity or less between 8 and 20 AU. The study presented here extends previous work by utilizing a larger statistical database and providing higher spatial resolution.

[32] The radial decay of the total energy per unit mass in the fluctuations is roughly a power law with an exponent of approximately $-1/2$. Assuming a constant flow velocity, this agrees with the result of *Biskamp and Müller* [2000] for the nonzero helicity case. This agreement is somewhat surprising considering that the effects of volume expansion in the solar wind are not taken into account in their simulations. This is one area of investigation for future research. The simulations by *Biskamp and Müller* [2000] also show that, in general, E^V decays faster than E^M as is found for the solar wind observations between 1 and 20 AU. It is probably fair to say that a complete understanding of the radial variation of the large-scale velocity and magnetic field fluctuations in the solar wind has not yet been

achieved. There is a continuing need for further development of theoretical models and more comprehensive in situ measurements.

[33] **Acknowledgments.** I would like to express my appreciation to D. Aaron Roberts for helpful discussions and for constructive comments on the initial manuscript. The spacecraft data used in this study were provided by the National Space Science Data Center (NSSDC) at Goddard Space Flight Center.

[34] Shadia Rifai Habbal thanks Eckart Marsch and Sean Oughton for their assistance in evaluating this paper.

References

Bavassano, B., and R. Bruno (1995), Density fluctuations and turbulent Mach numbers in the inner solar wind, *J. Geophys. Res.*, *100*, 9475.

Biskamp, D., and W.-C. Müller (2000), Scaling properties of three-dimensional isotropic magnetohydrodynamic turbulence, *Phys. Plasmas*, *7*, 4889.

Bridge, H. S., J. W. Belcher, R. J. Butler, A. J. Lazarus, A. M. Mavretic, and J. D. Sullivan (1977), The plasma experiment on the 1977 Voyager mission, *Space Sci. Rev.*, *21*, 259.

Bruno, R., and V. Carbone (2005), The solar wind as a turbulence laboratory, *Living Rev. Sol. Phys.*, *2*, 4.

Burlaga, L. F. (1995), *Interplanetary Magnetohydrodynamics*, Oxford Univ. Press, New York.

Burlaga, L. F., W. H. Mish, and D. A. Roberts (1989), Large scale fluctuations in the solar wind at 1 AU: 1978–1982, *J. Geophys. Res.*, *94*, 177.

Cranmer, S. R., and A. A. van Ballegooijen (2005), On the generation, propagation, and reflection of Alfvén waves from the solar photosphere to the distant heliosphere, *Astrophys. J. Suppl. Ser.*, *156*, 265.

Frisch, U. (1995), *Turbulence: The Legacy of A.N. Kolmogorov*, Cambridge Univ. Press, New York.

Goldstein, M. L., D. A. Roberts, and W. A. Matthaeus (1995), Magnetohydrodynamic turbulence in the solar wind, *Annu. Rev. Astron. Astrophys.*, *33*, 283.

Klein, L. W., L. F. Burlaga, and N. F. Ness (1987), Radial and latitudinal variations of the interplanetary magnetic field, *J. Geophys. Res.*, *92*, 9885.

Mariani, F., U. Villante, R. Bruno, B. Bavassano, and N. F. Ness (1979), An extended investigation of Helios 1 and Helios 2 observations: The interplanetary magnetic field between 0.3 and 1 AU, *Sol. Phys.*, *63*, 411.

Marsch, E. (1991), MHD turbulence in the solar wind, in *Physics of the Inner Heliosphere*, vol. 2, *Phys. Chem. Space*, vol. 20, edited by R. Schwenn and E. Marsch, p. 159, Springer, New York.

Marsch, E., and C.-Y. Tu (1990a), On the radial evolution of MHD turbulence in the inner heliosphere, *J. Geophys. Res.*, *95*, 8211.

Marsch, E., and C.-Y. Tu (1990b), Spectral and spatial evolution of compressible turbulence in the inner solar wind, *J. Geophys. Res.*, *95*, 11,945.

Matthaeus, W. H., G. P. Zank, C. W. Smith, and S. Oughton (1999), Turbulence, spatial transport, and heating of the solar wind, *Phys. Rev. Lett.*, *82*, 3444.

Roberts, D. A., and M. L. Goldstein (1991), Turbulence and waves in the solar wind, *Rev. Geophys.*, *29*(S), 932.

Roberts, D. A., M. L. Goldstein, and L. W. Klein (1990), The amplitudes of interplanetary fluctuations: Stream structure, heliocentric distance, and frequency dependence, *J. Geophys. Res.*, *95*, 4203.

Tu, C.-Y., and E. Marsch (1995), MHD structures, waves and turbulence in the solar wind: Observations and theories, *Space Sci. Rev.*, *73*, 1.

Zank, G. P., W. H. Matthaeus, and C. W. Smith (1996), Evolution of turbulent magnetic fluctuation power with heliospheric distance, *J. Geophys. Res.*, *101*, 17,093.

J. J. Podesta, Laboratory for Solar and Space Physics, NASA Goddard Space Flight Center, Code 612.2, Greenbelt, MD 20771, USA. (jpodesta@solar.stanford.edu)